Desalination and Water Treatment
www.deswater.com

doi: 10.1080/19443994.2016.1167127

57 (2016) 27061–27072
December

Taylor & Francis
Taylor & Francis Group

Analysis of two-parameter and three-parameter isotherms by nonlinear regression for the treatment of textile effluent using immobilized *Trametes versicolor*: comparison of various error functions

S. Vishali[a,*], P. Mullai[b]

[a]*Department of Chemical Engineering, SRM University, Chennai 603 203, India, Tel. +91 94438 83562; email: meet.vishali@gmail.com*
[b]*Faculty of Engineering and Technology, Department of Chemical Engineering, Annamalai University, Chidambaram 608 002, Tamil Nadu, India, Tel. +91 9486918357; email: pmullai@yahoo.in*

Received 10 December 2015; Accepted 12 March 2016

ABSTRACT

The ability of the immobilized *Trametes versicolor*, as biosorbent, to degrade the textile effluent, in terms of chemical oxygen demand and color, was studied under batch conditions. The removal efficiencies were calculated for the effect of initial concentrations, biomass dosages, shaking, and nutrients. Equilibrium data were analyzed using, two-parameter isotherms: Langmuir, Freundlich, BET, Flory–Huggins, Temkin, Jovanovic, Harkins–Jura and Halsey. Three-parameter isotherms: Redlich–Peterson, Sips, Khan, Toth, Langmuir–Freundlich, Fritz–Schlunder, Koble–Corrigan, Hill, Brouers–Sotolongo, and Radke Prausnitz, using nonlinear regression. The model parameters were optimized using Microsoft Excel Solver Add-Ins function. The best isotherm was identified by error analysis, using nine different error functions: residual root mean square error, normalized standard deviation, average relative error, sum of the squares of the error, sum of the absolute errors, hybrid fractional error function, residual variance, Marquardt's percent standard deviation, and chi-square test (χ^2).

Keywords: Textile effluent; Immobilized *Trametes versicolor*; Two-parameter isotherm models; Three-parameter isotherm models; Error functions

1. Introduction

Among the various available industries in the world, special attention is given to the textile industry because they often use dyes and pigments to color their products. From dyeing unit and subsequent unit operations, 10–20% of the dyes are lost in the wastewater [1]. The human eye can detect 0.005 mg/L of reactive dye in water [2]. The presence of excess amount of dye in the wastewater spoils the quality of water in the environment and affects the human health, and also aquatic cycle. The treatment of wastewater includes the degradation of dyestuff, removal of organic and inorganic components [3].

Many techniques have been developed for the dye removal such as ion exchange [4], electrochemical degradation [5], adsorption [6], advanced oxidation [7], coagulation and flocculation [8], membrane filtration [9], and so on. Due to the higher operative cost,

*Corresponding author.

sludge formation, the ineffectiveness of a broad range of dye removal identified in the above methods, made biosorption as the best alternative technology. Biosorption techniques are capable of removing the pollutants from the wastewater. It has many advantages like cost-effective, easy to operate, simple mechanism, and insensitive to pollutants [1].

Many authors have reported different types of adsorbents like, commercial activated carbon, carbon material made from solid wastes and coal-based sorbents like rice husk, waste newspaper, date pits, coir pith, sugarcane bagasse, neem sawdust, orange peel, banana pith, cotton waste, and natural materials like clay, glass powder, zeolite, and silica [10]. Biomasses including bacteria, fungi, yeast, both living and dead cells are used as biosorbent for the treatment of effluents. Researchers have observed in their recent studies that the ability of the micro-organisms to treat the wastewater from different industries like olive mill [11], distillery [12], antibiotic [13], paint [14], dairy [15], tannery [16], and heavy metals [17] too. Different micro-organisms are examined in the treatment of textile wastewater, like *Phanerochaete chrysosporium* [18], *Funalia trogii* [19], *Rhizopus arrhizus* [20], *Aspergillus wentii* [21], *Coriolus versicolor* [22], *Chlorella vulgaris* [23], and *Candida tropicalis* [24].

In this present study, the ability of the *Trametes versicolor*, a white rot fungus, for the treatment of textile wastewater has been evaluated by varying the operational parameters. The experimental values were fitted in the eight different types of two-parameter and 10 types of three-parameter isotherm models. Model parameters were calculated by nonlinear regression analysis and optimized by Excel Solver Add-Ins function. The best isotherm model was identified based on the error functions.

2. Materials and methods

2.1. Sorbent and sorbate

All chemicals used in the study were of analytical grade (AR). They were procured from Merck India. The textile effluent was collected from Veena Textiles Ltd, Erode, Tamil Nadu, India. The physicochemical characteristic of the sample was analyzed and the results are given in Table 1. *T. versicolor*, a fungal strain was obtained from National Chemical Laboratory (NCL), Pune, India.

2.2. Preparation of immobilized beads

Stock cultures of the strains were stored on the slants of potato dextrose agar at 4°C and periodically subcultured in dextrose agar medium, at 30°C for 7 d of incubation period. For the immobilization of *T. versicolor*, sodium alginite was used as a matrix. The cells formed were transferred aseptically to a sterile centrifuge tube and centrifuged at a speed of 10,000 rpm for 5 min. The known weight of biomass was added with 8% sodium alginate. The resultant slurry was extruded as drops into 2% calcium chloride solution, at room temperature, and strict aseptic condition was maintained while preparing the immobilized cells. The beads thus formed were hardened in the calcium chloride solution for an hour at room temperature. The size of the beads can be changed by altering the diameter of the injection needle used [8].

Table 1
The physicochemical characteristics of textile wastewater

Parameters	Concentration
pH	10
Color	Blackish
Odor	Odorless
COD (mg/L)	6,750
Total solids (mg/L)	112,100
Total dissolved solids (mg/L)	97
Total suspended solids (mg/L)	112,000

2.3. Experimental procedure

The known amount of biomass of *T. versicolour*, in an immobilized form, was added to 300 mL of textile effluent in the 500-mL Erlenmeyer flask. The chemical oxygen demand (COD) and the color removal efficiencies were calculated for every one hour till the equilibrium. The experiments were carried out to study the effect of operational parameters such as, different initial concentrations (200, 3,000, 4,000, 5,000, and 6,750 mg COD/L), biomass dosages (2, 3, 4, and 5 g), with and without shaking (100 rpm), and the presence and absence of nutrients such as glucose as carbon source, ammonium chloride as nitrogen source (5 g/L each).

Color measurements were done using ELICO SL 164 Spectrophotometer for the maximum absorbance (λ_{max}) of 405 nm. The percentage of color removal was calculated from the difference between the initial and final absorbance of textile effluent. COD measurements were carried out as described in standard methods [25]. The readings were taken in duplicate for an individual solution to check the repeatability and the average of the values were considered. The equilibrium adsorption of textile wastewater was calculated as follows (g/g):

$$q_e = \frac{(C_o - C_e)V}{W}$$

3. Theory

3.1. Equilibrium sorption models

The equilibrium of the process is often described by fitting the experimental points with models usually for the representation of adsorption equilibrium. The amount of material adsorbed is determined as a function of concentration at a constant temperature, and the resulting function is known as adsorption isotherm which provides an appropriate estimate of the adsorption capacity and intensity by adsorbents.

The adsorption capacity and the interaction between the textile effluent and the immobilized *T. versicolor* were determined by fitting the experimental values in the models. Models are used to analyze the experimental values. It gives the amount of pollutant removed from the effluent, at equilibrium, by a unit mass of biosorbent at constant temperature.

In the present study, equilibrium data were analyzed with eight different two-parameter isotherm models: Langmuir, Freundlich, BET, Flory–Huggins, Temkin, Jovanovic, Harkins–Jura and Halsey and 10 different three-parameter isotherm models: Redlich–Peterson, Sips, Khan, Toth, Langmuir–Freundlich, Fritz–Schlunder, Koble–Corrigan, Hill, Brouers–Sotolongo, and Radke–Prausnitz. Linearization of the model affects the normality of the least squares, and the distribution error changes either to best or worst. Due to this reason, all the above-mentioned models were solved using nonlinear regression analysis in Excel spreadsheet. The model parameters were optimized using Excel Solver Add-Ins function [26].

3.2. Error functions

The most suitable isotherm models were identified based on the error functions. The error functions are based on the equilibrium uptake values from the model and experiment. The best fit isotherm was selected based on the minimum error distribution between the predicted and experimental values. The smallest value of error functions will indicate the similarity of the model with the experimental data. In this study, complete error analysis was performed using nine different error functions: The residual root mean square error, normalized standard deviation, average relative error, Sum of the squares of the error, sum of the absolute errors, hybrid fractional error function, residual variance, Marquardt's percent standard deviation, and χ^2 test [27,28].

4. Results and discussions

4.1. Effect of initial concentration

For the five different initial concentrations of textile wastewater such as 6,750, 5,000, 4,000, 3,000, and 2,000 mg COD/L, the steady-state values of color removal efficiencies were 48.0, 50.33, 57.23, 64.3, and 100%, respectively, using 2 grams of *T. versicolour* under shaking at the end of the 20, 18, 13, 13, and 13th hour (Fig. 1a). In the case of 6,750 mg COD/L, the colour removal efficiency for the first three-hour was almost negligible due to the poor adsorption of the high concentration of dye. The equilibrium colour removal efficiency was 48.0% at the end of 20th hour. Complete colour removal of 100% was obtained at the end of 13th hour in the case of 2,000 mg COD/L due to the lower dye concentration.

The result clearly shows that the decrease in the dye concentration increased the color removal efficiency. Laccase a key enzyme from the *T. versicolour* is responsible for the color removal. The removals of dyes were increased with time till equilibrium was attained. At the beginning of the process, all the sites were vacant and hence the removal was high. Due to the limited vacant sites after the equilibrium level, there was no further increase in the decolourization efficiency. Similarly, 100% decolourization was observed on acid violet 7 with complex pellets of white rot fungus [29].

The corresponding COD removal efficiencies for the five different initial concentrations such as 6,750, 5,000, 4,000, 3,000, and 2,000 mg COD/L were 45.23, 52, 57, 63, and 68%, respectively, at the steady-state condition (Fig. 1b). The increase in the COD removal efficiency with respect to time is due to the well-acclimatized nature of the biomass with the effluent at the

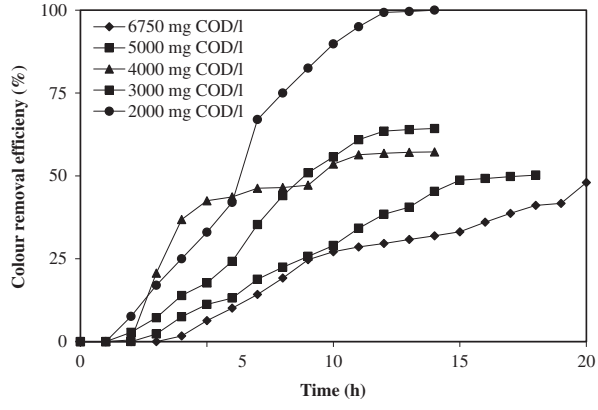

Fig. 1a. Effect of initial concentration on color removal efficiency.

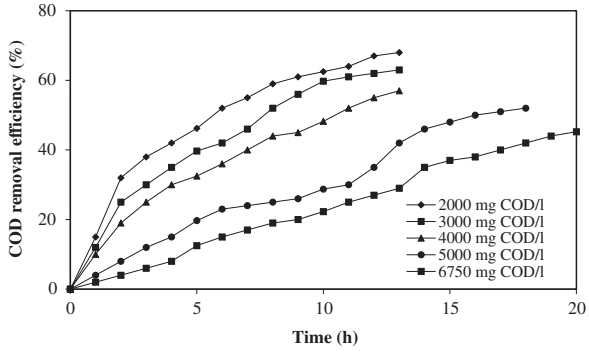

Fig. 1b. Effect of initial concentration on COD removal efficiency.

equilibrium condition. The studies on biodegradation of distillery wastewater using aerobic bacterial strains stated the similar results that the color removal efficiency increases with the COD reduction and remains almost parallel [30].

4.2. Effect of shaking

For the initial concentration of 2,000 mg COD/L, experiments were carried out with and without shaking condition. The steady-state color and COD removal efficiencies, respectively, were 100 and 68% under shaking at the end of 13th hour, and for without shaking was 100 and 63.12% at the end of 16th hour (Fig. 2).

Better results were attained under the shaking conditions and were much faster than the static condition. This is due to the better mass transfer efficiency, effective contact of effluent with the surface of the beads, and the good diffusion characteristics. It was confirmed that agitation was essential for keeping a high decolourization using *T. villosa* [31].

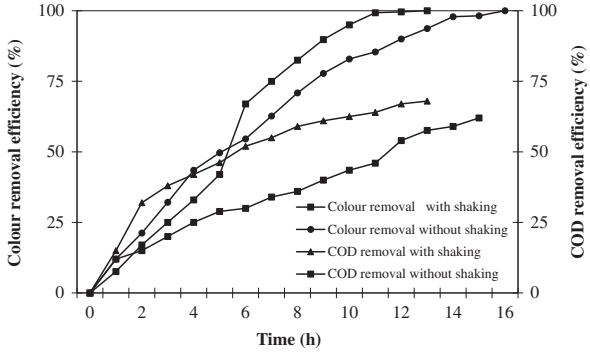

Fig. 2. Effect of shaking on color and COD removal efficiency.

4.3. Effect of nutrients

The initial concentration of 2,000 mg COD/L of textile effluent was treated, with and without the addition of 5 g/l of glucose as the carbon source, and ammonium chloride as a nitrogen source each. The equilibrium color and COD removal efficiencies, respectively, were 100 and 68% with the addition of nutrients at the end of the 11th hour and for without the addition of nutrients was 100 and 66.12% at the end of 13th hour (Fig. 3).

Though the equilibrium values attained in the case of addition of nutrients were faster and better, the difference was not appreciable. The result clearly indicates that the addition of nutrients does not significantly depress or stimulate the color and COD removal efficiency. Two findings were observed as that the enzyme secretion depends on nutrient limitation [32] and there was no significant influence of nutrient concentration on decolourization [33].

4.4. Effect of biomass dose

The experiment was repeated for the different dosage values of *T. versicolour* such as 2, 3, 4, and 5 g for 2,000 mg COD/L. The complete color removal was attained at the steady-state condition for all the four cases, and the equilibrium COD removal efficiencies were 68, 70.2, 74, and 79.2% at the end of 11, 11, 9, and 8th hour, respectively (Figs. 4a and 4b). Adsorption of dyes increased with the increase in biomass concentration, due to the availability of more active adsorbing sites. Further increase in biomass dosages brings about only marginal increase in color removal. The similar result was studied on the removal of copper from the effluent using fly ash [34].

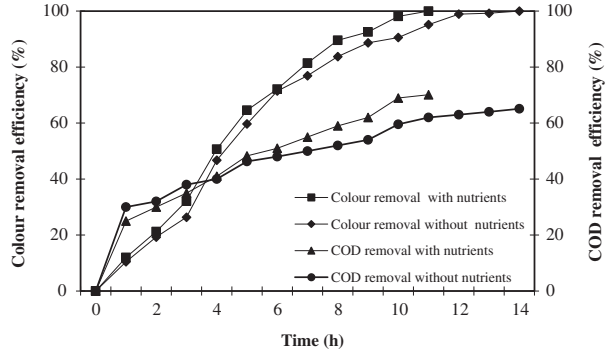

Fig. 3. Effect nutrients on color and COD removal efficiency.

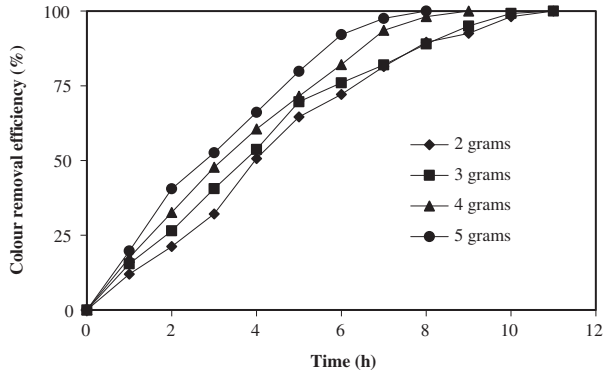

Fig. 4a. Effect of biomass dosage on color removal efficiency.

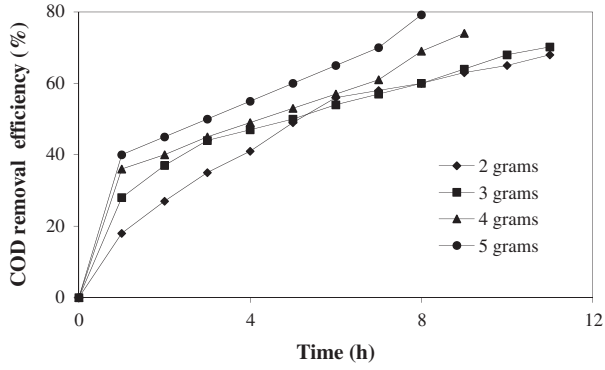

Fig. 4b. Effect of biomass dosage on COD removal efficiency.

4.5. Two-parameter isotherm models and error analysis

The equilibrium removal efficiencies increased with decrease in initial concentration, increase in biomass dosages, shaking, and in the absence of nutrients [35]. The effect of different concentrations and different biomass dosages on pollutant uptake by the sorbent was examined experimentally. These values were compared with the predicted equilibrium pollutant uptake from the eight different two-parameter isotherm models by nonlinear regression analysis. The optimized model parameters using Excel Solver Add-Ins function was tabulated in Table 2. All the models exhibits fairly good regression coefficient (R^2) values, that is greater than 0.9100.

For the Langmuir isotherm, the separation factor, R_L value indicates the behavior of the adsorption process. The R_L values were 0.1633 and 0.9959 for different concentration and dosages, respectively [14]. It confirms the favorable adsorption. $R_L = 1$ linear, $R_L < 0$ irreversible, $R_L > 1$ unfavorable, $0 < R_L < 1$ favorable. Over the entire dosage range, it was observed, the isotherm gave good linear correlation coefficient ($R^2 = 1$). It confirms that the data fit perfectly with the Langmuir isotherm [36].

This isotherm works on the assumption that firstly, there is monolayer coverage of the adsorbent surface by the pollutant molecules and secondly, that the surface is completely uniform and energetically homogeneous. In the present investigation, low values of k_L (<1) such as 0.002042, 0.7590 indicated high affinity of pollutant to *T. versicolor*. A high q_L (g/g) value 0.3123, 0.6133 illustrated the ability of *T. versicolor* to remove pollutants from the textile wastewater [37].

The Freundlich isotherm parameter $1/n_F$ measures the adsorption intensity of pollutant ions on adsorbent and Freundlich constant k_F is adsorption capacity [38]. $1/n_F$ values were 0.4333, 1.9690 for concentration, dosages, respectively, thereby indicating that adsorption took place through a physical process. These values also revealed greater heterogeneity of the adsorbent sites [39]. It is assumed that the stronger binding sites are occupied first and the binding strength decreases with the increasing degree of site occupation. It is originally empirical in nature, but was later interpreted as sorption to hetero surface or surface supporting sites of varied affinities [40].

The BET model assumes that a number of layers of adsorbate molecules are formed at the surface of sorbent and the Langmuir equation applies to each layer. A further assumption of the BET model is that a given layer need not complete formation prior to initiation of subsequent layers; the equilibrium condition will therefore involve several types of surfaces, in the sense of number of layers of molecules on each surface. B_{BET} is a constant which indicates the energy of interaction between the solute and the adsorbent surface, q_{BET} is an amount of solute adsorbed forming a complete monolayer (mg/g) [41].

The Florry–Huggins isotherm model gives the degree of surface coverage θ. The "n_{FH}" value indicates the greater number of pollutant occupying active sites of biomass. Larger "n_{FH}" value implies that more number of pollutants are occupying on the binding sites of adsorbents. The n_{FH} values are reasonably high (1.857 and 2.001). The equilibrium constant k_{FH} values are 4.022 and 0.9055 for dosage and concentration system, respectively. The larger value indicates the efficacy of biomass. The values suggested that the Florry–Huggins plot is favorable for dosage study and not for concentration study [41].

In Temkin, the heat of sorption of the molecules in layer decreases linearly with coverage due to sorbate and sorbent interactions. It assumes that the fall in the heat of sorption is more linear rather than the logarithmic heat of sorption of the molecules which decreases

Table 2
Parameters of two and three-parameter isotherms for different initial concentrations and biomass dosages

		Dosage	Conc.			Dosage	Conc.
Two-parameter isotherms							
Langmuir $q_e = \frac{q_L k_L C_e}{1+k_L C_e}$; $R_L = \frac{1}{1+k_L C_o}$	k_L	0.002042	0.7590	Freundlich $q_e = k_F C_e^{1/n_F}$	n_F	0.5079	2.308
	q_L	0.3123	0.6133		k_F	0.4456	0.264
	R_L	0.196696	0.1633		R^2	0.9967	0.9791
	R^2	1.0000	0.9209				
BET $q_e = \frac{B_{BET} C_e q_{BET}}{(C_o - C_e)(1+(B_{BET}-1)C_e/C_o)}$	B_{BET}	0.006134	2.700	Flory–Huggins $\frac{\theta}{C_o} = k_{FH}(1-\theta)^{n_{FH}}$; $\theta = 1 - C_e/C_o$	n_{FH}	1.857	2.001
	q_{BET}	42.95	0.2780		k_{FH}	4.022	0.9055
	R^2	0.9941	0.9951				
Temkin $q_e = \left(\frac{RT}{b_T}\right) \ln(k_T C_e)$	b_T	11,294	17,268	Jovanovic $q_e = q_J(1 - e^{k_J C_e})$	k_J	−0.4923	–0.65
	k_T	3.49	6.43		q_J	0.5132	0.5
	R^2	0.9965	0.9283		R^2	0.9998	0.9192
Harkins–Jura $q_e = \left[\frac{A_{HJ}}{B_{HJ} + \log C_e}\right]^{1/2}$	A_{HJ}	−0.0023	−0.0432	Halsey $q_e = e^{(\ln k_H - (\ln C_e)/n_H)}$	n_H	−0.5079	−2.54
	B_{HJ}	0.121	−0.667		k_H	1.5076	26.55
	R^2	0.9561	0.9508		R^2	0.9967	0.976
Three-parameter isotherms							
Redlich–Peterson $q_e = \frac{k_{RP} C_e}{1 + a_{RP} C_e^{b_{RP}}}$	k_{RP}	318	0.6075	Sips $q_e = q_{SIPS} \frac{(k_{SIPS} C_e)^{m_{SIPS}}}{1 + (k_{SIPS} C_e)^{m_{SIPS}}}$	q_{SIPS}	0.3446	0.7410
	a_{RP}	707	1.294		k_{SIPS}	0.1110	0.4838
	b_{RP}	0.9856	0.8472		m_{SIPS}	1.975	0.8125
	R^2	0.9966	0.9441		R^2	0.8336	0.9435
Khan $q_e = \frac{q_K b_K C_e}{(1+b_K C_e)^{a_K}}$	q_K	0.9744	0.3570	Toth $q_e = \frac{q_{TOTH} C_e}{(b_{TOTH} + C_e^{n_{TOTH}})^{(-1/n_{TOTH})}}$	q_{TOTH}	0.2067	0.0013
	a_K	96.16	0.7862		b_{TOTH}	0.6623	5,134
	b_K	0.00233	1.551		n_{TOTH}	1.270	1.790
	R^2	0.9998	0.9444		R^2	0.9986	1
Langmuir–Freundlich $q_e = \frac{k_{LF} C_e^{c_{LF}}}{(1+a_{LF} C_e^{c_{LF}})}$	k_{LF}	0.00069	0.4108	Fritz–Schlunder $q_e = \frac{q_{FS} k_{FS} C_e}{1 + q_{FS} C_e^{m_{FS}}}$	q_{FS}	6,099	1.294
	a_{LF}	1.002	0.5541		k_{FS}	0.4455	0.4696
	c_{LF}	0.01165	0.8124		m_{FS}	0.9688	0.8472
	R^2	0.9651	0.9435		R^2	0.9967	0.9441
Koble–Corrigan $q_e = \frac{A_{KC} C_e^{p_{KC}}}{(1+B_{KC} C_e^{p_{KC}})}$	A_{KC}	0.0006932	0.4108	Hill $q_e = \frac{q_{Hi} C_e^{n_{Hi}}}{k_{Hi} + C_e^{n_{Hi}}}$	q_{Hi}	772	0.7409
	B_{KC}	1.002	0.5542		k_{Hi}	1,582	1.803
	p_{KC}	0.01165	0.8124		n_{Hi}	2.132	0.8127
	R^2	0.9651	0.9435		R^2	0.9955	0.9435
Brouers–Sotolongo $q_e = q_{BS}\left(1 - e^{\left(-k_{BS} C_e^{n_{BS}}\right)}\right)$	q_{BS}	17.48	0.5846	Radke Prausnitz $q_e = a_R r_R C_e^{\beta_R} / a_R + r_R C_e^{\beta_{R-1}}$	a_R	7,908	0.6076
	k_{BS}	0.0257	0.5999		r_R	0.4456	0.4696
	n_{BS}	1.976	0.7101		β_R	1.969	0.1528
	R^2	0.9967	0.9448		R^2	0.9967	0.9441

linearly with coverage due to sorbate and sorbent interactions [36].

Wide range of R^2 (1–0.9192) is predicted from the two-parameter model. The highest value is one for the Langmuir isotherm followed by Jovanovic (0.9998), Halsey and Freundlich (0.9967), Temkin (0.9965), Harkins–Jura (0.9561), and BET (0.9941) for the different dosage study. For the different concentration study, the order followed by the model was BET (0.9951) > Freundlich (0.9791) > Halsey (0.9760) > Harkins–Jura (0.9508) > Temkin (0.9281) > Langmuir (0.9209) > Jovanovic (0.9192).

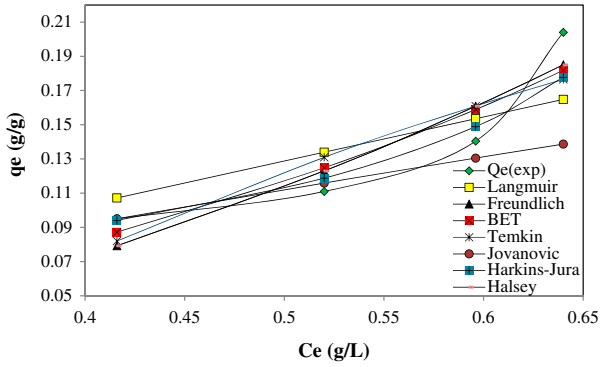

Fig. 5a. C_e vs. q_e for two-parameter isotherm-different dosages system.

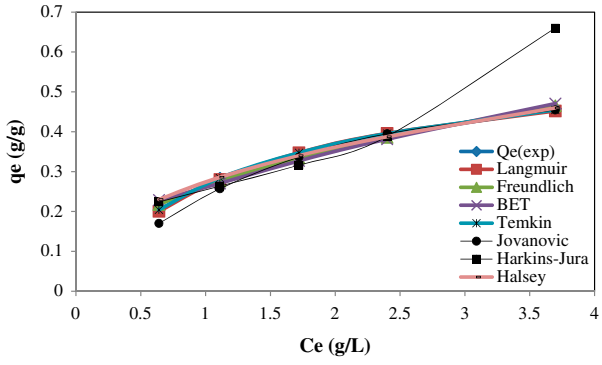

Fig. 5b. C_e vs. q_e for two-parameter isotherm-different concentrations system.

It is not necessary that the hierarchy of regression coefficient should match for different concentration and different dosage system. The adsorption rate depends on many parameters such as pollutant concentration, biomass dosage, and different operational conditions. The equilibrium uptake values predicted from the models were plotted and it was almost near to the experimental values shown in Figs. 5a and 5b.

R^2 value alone is not a factor to select the best model. In addition to this, nine different types of error analysis were adapted for this study, to check for better data fitness among the experimental and predicted equilibrium pollutant uptake values. All the error functions confirm the similarity between the experimental and predicted pollutant uptake by the positive, lowest, and zero nearer values. It means that the values from the model and experiment are expected to be equal. The values of the error functions indicate the deviation between these two.

All the error function equations (Table 3a) and its values for two-parameter isotherm models were listed in Table 3b for different dosages and concentration system. Under different dosages conditions, among the eight different models, Harkins–Jura exhibits the lowest value for nearly all the error function analysis. Jovanovic model shows the highest values for all the error function. Though R^2 values are good for the Jovanovic model and comparatively low for Harkins–Jura, based on the error functions it stands differently. Similarity between the experimental and predicted

Table 3a
Error functions

The residual root mean square error	RMSE	$\sqrt{\frac{1}{n-1}\sum_{n=1}^{n}\left(q_{e,exp}-q_{e,iso}\right)_n^2}$
Normalized standard deviation	NSD	$100\sqrt{\frac{1}{n-1}\sum_{n=1}^{n}\left(\frac{q_{e,exp}-q_{e,iso}}{q_{e,exp}}\right)_n^2}$
Sum of the squares of the error	ERRSQ	$\sum_{n=1}^{n}\left(q_{e,exp}-q_{e,iso}\right)_n^2$
Average relative error	ARE	$\frac{100}{n}\sum_{n=1}^{n}\left\|\frac{q_{e,exp}-q_{e,iso}}{q_{e,iso}}\right\|_n$
Sum of the absolute errors	EABS	$\sum_{n=1}^{n}\left\|q_{e,exp}-q_{e,iso}\right\|_{ni}$
Hybrid fractional error function	HYBRID	$\frac{100}{n-p}\sum_{n=1}^{n}\left[\frac{\left(q_{e,iso}-q_{e,exp}\right)^2}{q_{e,iso}}\right]_n$
Residual variance	S_{res}^2	$\frac{\sum_{n=1}^{n}\left(q_{e,exp}-q_{e,iso}\right)_n^2}{n-p}$
Marquardt's percent standard deviation	MPSD	$100\sqrt{\frac{1}{n-p}\sum_{i=1}^{n}\left(\frac{q_{e,iso}-q_{e,exp}}{q_{e,iso}}\right)_i^2}$
Chi-square test	χ^2	$\sum_{i=1}^{n}\left[\frac{q_{e,exp}-q_{e,iso}}{q_{e,exp}}\right]$

Table 3b
Error functions of two-parameter isotherms

Error functions	Langmuir	Freundlich	BET	Temkin	Jovanovic	Harkins–Jura	Halsey
Different dosages							
RMSE	0.0282	0.0197	0.0190	0.0241	0.0382	0.0166	0.0197
NSD	18.68	15.17	13.10	17.38	19.09	9.18	15.17
ARE	5.90	0.15	1.63	1.36	8.66	0.21	0.15
ERRSQ	2.38E–03	1.17E–03	1.09E–03	1.74E–03	4.39E–03	8.24E–04	1.17E–03
EABS	9.04E–03	2.35E–03	2.30E–03	2.65E–08	7.03E–02	1.10E–02	2.35E–03
HYBRID	7.870E–01	4.425E–01	3.548E–01	6.000E–01	1.585	2.445E–01	4.425E–01.
S^2_{res}	1.190E–03	5.847E–04	5.436E–04	8.718E–04	2.193E–03	4.121E–04	5.847E–04
MPSD	5.299E–02	3.793E–02	2.438E–02	4.446E–02	1.146E–01	1.476E–02	3.793E–02
χ^2	1.505E–02	8.650E–03	7.218E–03	1.207E–02	2.182E–02	4.455E–03	8.650E–03
Different concentrations							
RMSE	0.0054	0.0097	0.0176	0.0040	0.0219	0.1028	0.0133
NSD	1.612	3.880	7.059	1.083	9.582	23.183	6.475
ARE	0.1994	0.4471	0.7580	0.5011	5.3932	7.7944	2.6053
ERRSQ	1.182E–04	3.732E–04	1.235E–03	6.557E–05	1.912E–03	4.231E–02	7.100E–04
EABS	1.149E–03	1.280E–03	1.060E–03	8.060E–03	6.406E–02	1.748E–01	2.640E–02
HYBRID	1.126E–02	4.649E–02	1.502E–01	5.746E–03	3.212E–01	2.242E	1.019E–01
S^2_{res}	3.942E–05	1.244E–04	4.117E–04	2.186E–05	6.374E–04	1.410E–02	2.367E–04
MPSD	1.865	4.298	7.590	1.236	12.995	19.494	6.632
χ^2	3.381E–04	1.443E–03	4.777E–03	1.744E–04	8.264E–03	9.450E–02	3.443E–03

values was fitted well for the Harkins–Jura and deviations are comparatively wider for the Jovanovic. Other models are lying between these models. For the different concentration conditions, almost all the error function values are lowest one for the Temkin model, and entire values were higher for the Harkins–Jura model, remaining model lies between these two.

4.6. Three-parameter isotherm models and data fitness

Redlich–Peterson is a hybrid three-parameter isotherm, which combined the parameter of both Langmuir and Freundlich isotherms. It can be used for both homogeneous and heterogeneous systems. If the exponent component b_{RP} lies between 0 and 1, then the model supported the heterogeneous system of sorption. The b_{RP} values are 0.9856, 0.8472 and it confirms the heterogeneous nature [37,38].

In Sips isotherm, k_{SIPS} is the Sips model isotherm constant (L/mg), q_{SIPS} is the maximum monolayer biosorption (g/g), and m_{SIPS} the exponent of the model [1]. The Sips model constant k_{SIPS} and Sips model exponent m_{SIPS} were close to unity implying that the pollutant was taken by the functional groups or binding sites on the surface of the *T. versicolour* [37]. Sips isotherm provides rationally accurate prediction of textile wastewater with experimental results showing high R^2 values. It was also derived from the

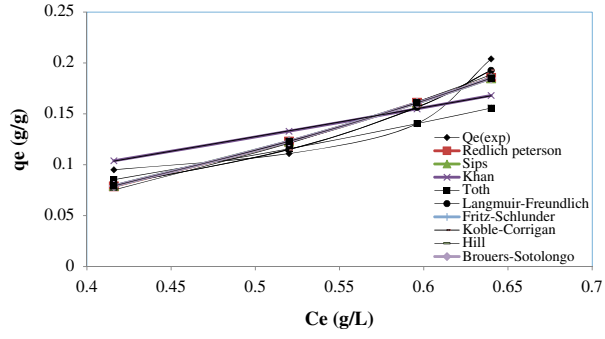

Fig. 6a. C_e vs. q_e for three-parameter isotherm-different dosages system.

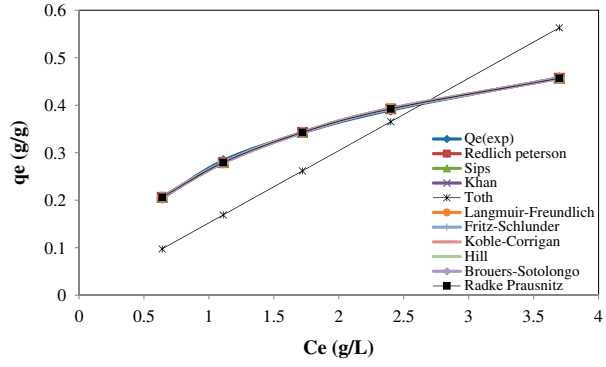

Fig. 6b. C_e vs. q_e for three-parameter isotherm-different concentrations system.

Table 3c
Error functions of three-parameter isotherms

Error functions	Redlich peterson	Sips	Khan	Toth	Langmuir–Freundlich	Fritz–Schlunder	Koble–Corrigan	Hill	Brouers–Sotolongo	Radke Prausnitz
Different dosages										
RMSE	0.01975	0.01976	0.02622	0.02858	0.01441	0.01974	0.01441	0.01998	0.01976	0.01974
NSD	15.28	15.17	17.27	15.09	11.84	15.17	11.84	16.43	15.18205	15.17326
ARE	0.2528	0.1963	5.4487	7.4099	1.5389	0.1523	1.5389	1.0216	0.2000	0.1504
ERRSQ	1.170E–03	1.172E–03	2.063E–03	2.451E–03	6.226E–04	1.169E–03	6.226E–04	1.198E–03	1.172E–03	1.169E–03
EABS	2.606E–03	2.668E–03	9.367E–03	5.330E–02	6.061E–03	2.391E–03	6.061E–03	3.787E–03	2.647E–03	2.372E–03
HYBRID	0.89528	0.88665	1.34252	1.62913	0.52201	0.88502	0.52201	1.01938	0.88771	0.88521
S^2_{res}	1.170E–03	1.172E–03	2.063E–03	2.451E–03	6.226E–04	1.169E–03	6.226E–04	1.198E–03	1.172E–03	1.169E–03
MPSD	27.90	27.57	29.84	33.30	22.32	27.54	22.32	31.74	28	28
χ^2	8.713E–03	8.653E–03	1.300E–02	1.263E–02	4.942E–03	8.648E–03	4.942E–03	9.522E–03	8.661E–03	8.650E–03
Different concentrations										
RMSE	0.002670	0.0031	0.0025	0.1032	0.0031	0.0027	0.0031	0.0031	0.0035	0.0027
NSD	0.9510	1.081	0.8951	37.02	1.082	0.9513	1.082	1.081	1.267	0.9512
ARE	0.04224	0.0410	0.0407	19.9	0.0409	0.0419	0.0409	0.0408	0.0599	0.0423
ERRSQ	2.852E–05	3.855E–05	2.475E–05	4.261E–02	3.855E–05	2.852E–05	3.855E–05	3.855E–05	4.998E–05	2.852E–05
EABS	1.304E–04	9.927E–05	1.147E–04	2.209E–01	9.915E–05	1.240E–04	9.915E–05	9.714E–05	1.582E–04	1.292E–04
HYBRID	4.991E–03	6.594E–03	4.377E–03	1.202E+01	6.597E–03	4.992E–03	6.597E–03	6.591E–03	8.795E–03	4.991E–03
S^2_{res}	1.426E–05	1.928E–05	1.238E–05	2.130E–02	1.928E–05	1.426E–05	1.928E–05	1.928E–05	2.499E–05	1.426E–05
MPSD	1.351146	1.537	1.271	94.67	1.538	1.352	1.538	1.537	1.8007	1.351
χ^2	9.928E–05	1.311E–04	8.711E–05	1.466E–01	1.311E–04	9.931E–05	1.311E–04	1.310E–04	0.0002	0.0001

Langmuir–Freundlich isotherm models. The maximum uptake was 0.3446 and 0.7410 g/g for different dosages and initial concentrations, respectively.

In the Khan model b_K is the constant and a_K is an exponent. The maximum uptake values q_K were well predicted by the model with relatively high correlation coefficients. A generalized model suggested for the pure solution is Khan isotherm, with the model constants and model exponent. It gives the better R^2 (0.9988) value [28,38].

Toth isotherm model was used in the present study to throw light on the heterogeneous sorption systems in play. It could be successfully applied to both low and high concentration of adsorbates. The model constant values revealed the heterogeneity of adsorbent surface [37]. It is empirically derived to improve the fitness of the model with experimental data. The correlation coefficient was 0.9986 and 1. Though the R^2 value was 1 for the different initial concentration system the q_T was 0.0013 g/g. Toth model was comparatively not suited for different concentration system, and holds good for the different dosages condition with q_T of 0.2026 g/g.

Koble–Corrigan has an exponential depending on the concentration in the numerator and denominator, which is usually used with heterogeneous sorption surfaces. The low values of p, 0.01165 and 0.8124 (less than 1) suggested that the sorption of pollutants in textile wastewater on *T. versicolor* is heterogeneous [37]. The correlation coefficient R^2 values ranged from 0.9998 to 0.8336 for various dosages and it was from 1 to 0.9435 for different concentrations. The q_e values from the models overlapped with the theoretical q_e values shown in Figs. 6a and 6b.

Khan and Toth isotherms were found better compared with other models. The model parameters are listed in Table 2. The order followed by the model was Different dosages: Khan (0.9998) > Toth (0.9986) > Fritz–Schlunder, Brouers–Sotolongo, Radke Prausnitz (0.9967) > Redlich–Peterson (0.9966) > Hill (0.9955) > Langmuir–Freundlich, Koble–Corrigan (0.9651) > Sips (0.8336) Different oncentrations: Toth (1) > Brouers–Sotolongo (0.9448) > Khan (0.9444) > Fritz–Schlunder, Radke Prausnitz, Redlich–Peterson (0.9441) > Sips, Langmuir–Freundlich, Koble–Corrigan, Hill (0.9435).

The deviation and the similarity between the predicted and experimental values were checked through the error function analysis. Based on the least values, the best isotherms were chosen. All the models are showing the minimum values of the error functions (Table 3c) among which the Langmuir–Freundlich, Koble–Corrigan, Khan models were observed better compared with other models, because it gave the lowest value among the available models, for all the nine error analysis. The deviations were comparatively high for the Toth isotherm, both under various concentration and dosages conditions. Though the R^2 value was favorable for the Toth isotherm, error analysis clearly shows its inability to match with the experimental values. The error functions were based on the experimental and calculated q_e values from the model values, number of parameters in the isotherm, and number of measurements taken [42].

5. Conclusions

This paper ascertained that the immobilized beads of *T. versicolor* could be efficiently used as a biosorbent for the treatment of textile industry wastewater. The experimentally found equilibrium pollutant uptake was compared with theoretically calculated q_e values of eight different two-parameter model and nine different three-parameter models. Based on the regression coefficient, Langmuir and BET, Khan and Toth isotherms showed better equilibrium fit among the two-parameter and three-parameter models, respectively. Model values confirmed that the system is heterogeneous in nature and the adsorption is physical in nature. Model parameters are evaluated by nonlinear regression analysis and optimized by Excel Solver Add-Ins function. Using the ten different error functions, best isotherms were selected, they are: Harkins–Jura, Temkin, Langmuir–Freundlich, Koble–Corrigan, and Khan Isotherms. In terms of both R^2 and error functions, Khan Isotherm was the best to represent the equilibrium experimental data.

Nomenclature

$q_{e,exp}$	—	equilibrium uptake of pollutants from the experiment (g/g)
$q_{e,iso}$	—	equilibrium uptake of pollutants from the isotherm model (g/g)
n	—	number of measurements
p	—	number of parameters present in the model
C_0, C_e	—	initial and equilibrium solution concentrations (g/L)
V	—	volume of the wastewater (L)
W	—	weight of the biomass used (g)
R^2	—	correlation coefficient
R_L	—	separation factor

References

[1] G.L. Dotto, E.C. Lima, L.A.A. Pinto, Biosorption of food dyes onto *Spirulina platensis* nanoparticles: Equilibrium isotherm and thermodynamic analysis, Bioresour. Technol. 103(1) (2012) 123–130.

[2] K. Santhy, P. Selvapathy, Removal of reactive dyes from wastewater by adsorption on coir pith activated carbon, Bioresour. Technol. 97 (2006) 1329–1336.
[3] A. Özcan, A.S. Özcan, Adsorption of acid red 57 from aqueous solution onto surfactant-modified sepiolite, J. Hazard. Mater. 125 (2005) 252–259.
[4] S. Karcher, A. Kornmüller, M. Jekel, Anion exchange resins for removal of reactive dyes from textile wastewaters, Water Res. 36(19) (2002) 4717–4724.
[5] K.B. Korbahti, A. Tanyolac, Continuous electrochemical treatment of simulated industrial textile wastewater from industrial components in a tubular reactor, J. Hazard. Mater. 170(2–3) (2009) 771–778.
[6] S. Vishali, P. Rashmi, R. Karthikeyan, Potential of environmental-friendly, agro-based material *Strychnos potatorum*, as an adsorbent, in the treatment of paint industry effluent, Desalin. Water Treat. (2015), doi: 10.1080/19443994.2015.1091990.
[7] J.P.V. Vilar, X.L. Pinho, M.A.A. Pintor, A.R.R. Boaventura, Treatment of textile wastewaters by solar-driven advanced oxidation processes, Sol. Energy 85(9) (2011) 1927–1934.
[8] S. Vishali, R. Karthikeyan, A comparative study of strychnos potatorum and chemical coagulants in the treatment of paint and industrial effluents: An alternate solution, Sep. Sci. Technol. 49(16) (2014) 2510–2517.
[9] E. Kurt, D. Yuksel, K. Imer, N. Dizge, S. Chellam, I. Koyuncu, Pilot-scale evaluation of nanofiltration and reverse osmosis for process reuse of segregated textile dyewash wastewater, Desalination 302(17) (2012) 24–32.
[10] C. Gregorio, Non-conventional low cost adsorbents for dye removal: A review, Bioresour. Technol. 97 (2006) 1061–1085.
[11] A. Lamia, H. Moktar, Fermentative decolourization of olive mill wastewater by *Lactobacillus plantarum*, Process Biochem. 39 (2003) 59–65.
[12] D. Pant, A. Adholeya, Biological approaches for treatment of distillery wastewater: A review, Bioresour. Technol. 98(12) (2007) 2321–2334.
[13] P. Mullai, S. Vishali, Biodegradation of Pencillin–G wastewater using *Phanerachate chrysosporium*-An equilibrium and kinetic modeling, Afr. J. Biotechnol. 6(12) (2007) 1450–1457.
[14] M. Malakootian, J. Nouri, H. Hossaini, Removal of heavy metals from paint industry's wastewater using Leca as an available adsorbent, Int. J. Environ. Sci. Technol. 6(2) (2009) 183–190.
[15] J.P. Kushwaha, V.C. Srivastava, I.D. Mall, Treatment of dairy wastewater by commercial activated carbon and bagasse fly ash: Parametric, kinetic and equilibrium modelling, disposal studies, Bioresour. Technol. 101 (2010) 3474–3483.
[16] R. Baccar, P. Blánquez, J. Bouzid, M. Feki, H. Attiya, M. Sarrà, Modeling of adsorption isotherms and kinetics of a tannery dye onto an activated carbon prepared from an agricultural by-product, Fuel Process. Technol. 106 (2013) 408–415.
[17] K. Tsekova, D. Todorova, V. Dencheva, S. Ganeva, Biosorption of copper(II) and cadmium(II) from aqueous solutions by free and immobilized biomass of Aspergillus niger, Bioresour. Technol. 101 (2010) 1727–1731.
[18] M.M. Assadi, K. Rostami, M. Shahvali, M. Azin, Decolorization of textile wastewater by *Phanerochaete chrysosporium*, Desalination 141(3) (2001) 331–336.
[19] O. Yesilada, S. Cing, D. Asma, Decolourisation of the textile dye Astrazon Red FBL by *Funalia trogii* pellets, Bioresour. Technol. 81(2) (2002) 155–157.
[20] Z. Aksu, S. Sen, C.F. Gonen, Continuous fixed bed biosorption of reactive dyes by dried *Rhizopus arrhizus*: Determination of column capacity, J. Hazard. Mater. 143(1–2) (2007) 362–371.
[21] Y. Khambhaty, K. Mody, S. Basha, Efficient removal of Brilliant Blue G (BBG) from aqueous solutions by marine *Aspergillus wentii*: Kinetics, equilibrium and process design, Ecol. Eng. 41 (2012) 74–83.
[22] M. Asgher, N. Azim, H.N. Bhatti, Decolorization of practical textile industry effluents by white rot fungus *Coriolus versicolor* IBL-04, Biochem. Eng. J. 47(1–3) (2009) 61–65.
[23] S.L. Lim, W.L. Chu, S.M. Phang, Use of *Chlorella vulgaris* for bioremediation of textile wastewater, Bioresour. Technol. 101 (2010) 7314–7322.
[24] D. Charumathi, N. Das, Packed bed column studies for the removal of synthetic dyes from textile wastewater using immobilised bead *C. tropicalis*, Desalination 285 (2012) 22–30.
[25] APHA, Standard Methods for the Examination of Water and Wastewater, twentieth ed., American Public Health Association, American Water Works Association and Water Pollution Control Federation, Washington, DC, 1955.
[26] K. Vasanthkumar, K. Porkodi, F. Rocha, Isotherms and thermodynamics by linear and non-linear regression analysis for the sorption of methylene blue onto activated carbon: Comparison of various error functions, J. Hazard. Mater. 1511 (2008) 794–804.
[27] M. Barkat, D. Nibou, S. Chegrouche, A. Mellah, Kinetics and thermodynamics studies of chromium(VI) ions adsorption onto activated carbon from aqueous solutions, Chem. Eng. Process. 48 (2009) 38–47.
[28] K.Y. Foo, B.H. Hameed, Insights into the modeling of adsorption isotherm systems, Chem. Eng. J. 156 (2010) 2–10.
[29] F. Zhang, J. Yu, Decolourisation of acid violet 7 with complex pellets of white rot fungus and activated carbon, Bioprocess. Eng. 23 (2000) 295–301.
[30] C. Nanjundasamy, P. Kumar, N. Jain, Biodegradation of predigested distillery wastewater by aerobic bacterial strains, Ind. J. Environ. Prot. 18(9) (1998) 658–661.
[31] C.H.L. Soares, N. Duran, Degradation of low and high molecular mass fractions of kraft effluent by *T. villosa*, Environ. Technol. 19 (1998) 883–891.
[32] I. Kapdan, G. Mcmullan, F. Kargi, Comparision of white rot fungi cultures for decolorization of textile dyestuffs, Bioprocess Eng. 22 (1999) 347–351.
[33] F. Yuzhu, T. Viraraghavan, Fungal decolourization of dye wastewater, Bioresour. Technol. 79 (2001) 251–262.
[34] M.P. Kapadia, R.P. Farasvam, M.M. Bhatt, Removal of copper from effluent by flyash, Ind. J. Environ. Prot. 20(7) (2000) 521–528.
[35] P. Mullai, S. Vishali, Application of *Trametes veriscolor* in the degradation of textile wastewater, Int. J. Chem. Sci. 8(5) (2010) S224–S232.
[36] E. Bulut, M. Özacar, A.I. Şengil, Adsorption of malachite green onto bentonite: Equilibrium and kinetic studies and process design, Microporous Mesoporous Mater. 115 (2008) 234–246.

[37] M.A. Hossain, H.H. Ngo, W.S. Guo, T.V. Nguyen, Palm oil fruit shells as biosorbent for copper removal from water and wastewater: Experiments and sorption models, Bioresour. Technol. 113 (2012) 97–101.
[38] K. Vijayaraghavan, T.V.N. Padmesh, K. Palanivelu, M. Velan, Biosorption of Nickel(II) ions onto *Sargassum wightii*: Application of two-parameter and three-parameter isotherm models, J. Hazard. Mater. 133 (2006) 304–308.
[39] J.P. Kushwaha, V.C. Srivastava, I.D.D. Mall, Treatment of dairy wastewater by commercial activated carbon and bagasse fly ash: Parametric, kinetic and equilibrium modelling, disposal studies, Bioresour. Technol. 101 (2010) 3474–3483.
[40] M. Akhtar, S. Iqbal, M.I. Bhanger, Z.U.M. Haqc, M.M. Moazzamd, Sorption of organophosphorous pesticides onto chickpea husk from aqueous solutions, Colloids Surf. B 69 (2009) 63–70.
[41] R. Nadeem, M.H. Nasir, M.S. Hanif, Pb (II) sorption by acidically modified *Cicer arientinum* biomass, Chem. Eng. J. 150 (2009) 40–48.
[42] R. Krishna, S.N. Prasad, Srivastava, sorption of distillery spent wash onto fly ash: Kinetics and mass transfer studies, Chem. Eng. J. 16 (2009) 90–97.